ELSEVIER

Microelectronics Journal **28** (1997) 183–198

0026-2692/97/$17.00

PII:S0026-2692(96)00061-4

Review paper

Monte Carlo analysis of electronic noise in semiconductor materials and devices

L. Reggiani[1], P. Golinelli[2], L. Varani[3], T. González[4], D. Pardo[4], E. Starikov[5], P. Shiktorov[5] and V. Gružinskis[5]

[1]*Istituto Nazionale di Fisica della Materia, Dipartimento di Scienza dei Materiali, Università di Lecce, Via Arnesano, I-73100 Lecce, Italy*
[2]*Istituto Nazionale di Fisica della Materia, Dipartimento di Fisica, Università di Modena, Via Campi 213/A, I-41100 Modena, Italy*
[3]*Centre d'Electronique et de Microoptoelectronique de Montpellier (CNRS UMR 5507), Université des Sciences et Techniques du Languedoc, F-34095 Montpellier Cedex 5, France*
[4]*Departamento de Física Aplicada, Universidad de Salamanca, Plaza de la Merced s/n, E-37008 Salamanca, Spain*
[5]*Semiconductor Physics Institute, Goshtauto 11, 2600 Vilnius, Lithuania*

We review recent results concerning the microscopic analysis of electronic noise in semiconductor unipolar structures in the frequency range where $1/f$ noise can be neglected. Calculations are based on a Monte Carlo simulator of the carrier motion self-consistently coupled with a Poisson solver. Both current– and voltage–noise operation modes are considered and their respective advantages illustrated. The analysis is applied to structures with increasing degree of complexity, that is: homogeneous materials, resistors, n^+nn^+ diodes, Schottky-barrier diodes and GaAs MESFETs. The main sources of noise like diffusion, generation–recombination, coupling between velocity and local electric field fluctuations, etc. are treated in the presence of electric fields of arbitrary strength. Results should constitute the basis for a physical interpretation of electronic noise in most semiconductor materials and devices thus providing inputs for improving quality and reliability figures of merit.

1. Introduction

Electronic noise represents both an intrinsic limit to the performances of devices and a valuable quantity to get information on the

transport characteristics of the specimen of interest. For a systematic documentation the reader is sent to a periodic series of International Noise Conferences, the last of them being reported in [1–8]. It is important to remark that, under biasing conditions associated with an external applied voltage, noise spectra provide in general complementary information with respect to transport spectra given by small-signal response parameters like differential impedance and/or admittance. In particular, all types of noise (i.e. diffusion, generation recombination, shot, $1/f$, etc.) play a role in figuring out the quality and reliability of devices by offering a non-invasive experimental technique [9].

Despite its recognized importance, the microscopic interpretation of noise spectra at a kinetic level is a complicated affair because of the difficulties in solving the appropriate master equation [10, 11]. As a consequence, when compared with the interpretation of first order quantities (i.e. current-voltage characteristics and related parameters), that of second-order quantities is found to be unsatisfactory in many instances. The most illuminating example is the coupling between fluctuations in carrier velocities (or number) with those in local electric field, which is usually treated on a phenomenological level making use of an equivalent-circuit analysis with appropriate voltage and current noise generators distributed ad hoc. A second valuable example is the usual accepted procedure of assuming the decoupling approximation. It consists of decomposing the total noise in terms of different sources by means of which the total spectrum is written as a sum of individual noise sources thus neglecting cross-correlation contributions [12].

We believe that a breakthrough in the microscopic modelling of noise has arisen with the application of the Monte Carlo (MC) simulation technique [13–17]. In a seminal paper of 1980, Zimmermann and Constant [18] showed the basis of such an application. Starting from that date, several researchers have applied and implemented this technique [19–55], which is now recognized as one of the most powerful methods for giving an exact solution of the appropriate master equation. On the basis of a joint collaboration inside the network of excellence European Laboratory for Electronic Noise (ELEN) supported by the European Community, we have analyzed a variety of physical situations which we consider of sufficient interest for the researchers working in the field of semiconductor microelectronics.

The aim of this paper is thus to briefly review some of the most interesting results we have recently obtained by using the MC technique coupled with a Poisson solver. The main issues which will be addressed are: (i) to present the general theory; (ii) to investigate systems with increasing degree of complexity; (iii) to develop a theoretical modeling of the device noise–temperature. In this way we will provide the general reader with a microscopic interpretation which accounts for the basic physics and as such is directly transferable to the device of interest. Limitation in space does not allow us to provide many details which, however, can be found in the cited literature. Finally, we point out that the present analysis is limited to frequencies sufficiently high so that $1/f$ noise can be neglected.

2. Theory

The primary quantities describing electronic noise are the spectral density of current or voltage fluctuations, $S_I(f)$ and $S_V(f)$, respectively. They can be measured more or less directly in different ranges of the frequency f and microscopically interpreted from the calculation of their theoretical counterparts which are the associated correlation functions $C_I(t)$ and $C_V(t)$, respectively. Accordingly, in studying electronic noise two different modes of operation, which are mutually exclusive, can be used, namely: current- and voltage-noise operation mode. (A third circuit-noise operation mode, intermediate

between the two cited above, has been recently proposed [55].) In the former, the voltage drop at the terminals of the device is kept constant in time and the current fluctuations in the external short circuit are analyzed. In the latter, the current in the device is kept constant in time and the voltage fluctuations at its terminals are analyzed. Both modes are of interest since, as will be illustrated in the forthcoming, they provide different and complementary information. We remark that from a small-signal circuit analysis the two spectral densities are interrelated by:

$$S_V(f) = |Z(f)|^2 S_I(f) \tag{1}$$

$Z(f)$ being the small-signal impedance of the device under test. (Some attention should be paid in using the above equation in proximity of unstable conditions such as those associated with the Gunn effect [55].)

If X is the current or the voltage then, from the Wiener–Khintchine theorem [56], it is:

$$S_X(f) = 2\int_{-\infty}^{+\infty} \exp(i2\pi ft) C_X(t)\,\mathrm{d}t \tag{2}$$

$$C_X(t) = \overline{\delta X(t')\delta X(t'+t)} \tag{3}$$

where $\delta X(t) = X(t) - \overline{X}$ is the fluctuation of X around its average value $\overline{X}$. Here we assume ergodicity and take the bar as synonymous of time average. The theoretical problem remains to provide a microscopic calculation of $C_X(t)$. The theory underlying the above noise operations is briefly summarized in the following for the semiclassical case when a single type of carrier (electrons or holes) is present. Provided the length of the device is small compared to its lateral dimensions, the flux of the displacement current density through the lateral surfaces can be neglected and a one-dimensional treatment can be applied. By neglecting magnetic effects, which for devices operating up to the microwave range (i.e. $f \leqslant 300$ THz) is always well justified, the total current through each cross-sectional area is the same and given by the Ramo–Shockley theorem [57, 58] and its generalization [59] as:

$$I(t) = \frac{e}{L}\sum_{i=1}^{N_T(t)} v_i(t) - \varepsilon_0\varepsilon_r \frac{A}{L}\frac{\mathrm{d}}{\mathrm{d}t}[V(L,t) - V(0,t)] \tag{4}$$

where e is the absolute value of the electronic charge, L and A the length and cross-sectional area of the sample, respectively, v_i the instantaneous value of the velocity component in the field direction of the ith carrier, $N_T(t)$ the total number of carriers which are instantaneously present in the sample, ε_0 the vacuum permittivity, and ε_r the relative static dielectric constant of the background medium. Under current noise-operation $\mathrm{d}/\mathrm{d}t[V(L,t) - V(0,t)] = 0$ and eq. (4) gives:

$$I(t) = \frac{e}{L}\sum_{i=1}^{N_T(t)} v_i(t) = \frac{e}{L} N_T(t) v_d(t) \tag{5}$$

where $v_d(t) = [1/N_T(t)]\sum_{i=1}^{N_T(t)} v_i(t)$ is the drift velocity. Under voltage noise operation $I(t) = I_0 = \text{const}$ and the time derivative of the voltage drop at the contacts $\Delta V(t) = [V(L,t) - V(0,t)]$ is calculated as:

$$\frac{\mathrm{d}}{\mathrm{d}t}\Delta V(t) = \frac{L}{A\varepsilon_0\varepsilon_r}\left[\frac{e}{L}\sum_{i=1}^{N_T(t)} v_i(t) - I_0\right] \tag{6}$$

Then, $\Delta V(t)$ can be obtained from a numerical integration of eq. (6) [37]. In practice, the determination of $C_X(t)$ is performed from the knowledge of the time series $X(t)$ as calculated from an ensemble MC simulation eventually coupled with a self-consistent Poisson solver, and taking appropriate boundary conditions concerning carrier injection–extraction from the contacts of the device. We remark that the stochastic nature of $X(t)$ comes from the microscopic collision rates describing scattering of carriers with different scatterer centers (i.e. phonons, impurities, other carriers, etc.). Thus,

the simulation provides both average values and fluctuations around the steady-state in a natural way without introducing any ad hoc assumptions. At high frequencies (typically $f >$ 10 MHz), the measurement of the device noise–temperature, $T_n(f)$, being a direct output of experiments [60], is often used as a method to investigate electronic noise. Its definition comes from the use of a generalized Nyquist relation in the form [61]:

$$T_n(f) = \frac{S_I(f)}{4K_B \mathrm{Re}[Y(f)]} = \frac{S_V(f)}{4K_B \mathrm{Re}[Z(f)]} \qquad (7)$$

where K_B is the Boltzmann constant, and $\mathrm{Re}[Y(f)]$ and $\mathrm{Re}[Z(f)]$ the real part of the small-signal admittance and impedance at the bias point, respectively. (Notice that the above definition requires the constraint $\mathrm{Re}[Y(f)] > 0$ or $\mathrm{Re}[Y(f)] > 0$.) Since both $S_I(f)$ and $Y(f)$ (or $S_V(f)$ and $Z(f)$) can be theoretically evaluated with a MC or a mixed MC hydrodynamic approach [55], $T_n(f)$ can be evaluated through eq. (7). In the following we report the results obtained by applying the MC technique to different systems with increasing degree of complexity.

3. Homogeneous material

The system we consider is lightly doped p-type Si at 77 K [41] where, because of partial freeze-out, only a fraction of acceptors is ionized at thermodynamic equilibrium. Under these conditions, in addition to thermal noise, generation–recombination noise contributes significantly to the total noise in the presence of an external field. Figure 1 reports the current spectral densities for the three significative fields and two acceptor concentrations. Theory well reproduces the main features of experiments and agrees with them within factor 2 at worst. At the lowest frequencies generation and recombination mechanisms originate an excess noise which adds to free carrier velocity fluctuations and is responsible for the large value of the plateau at

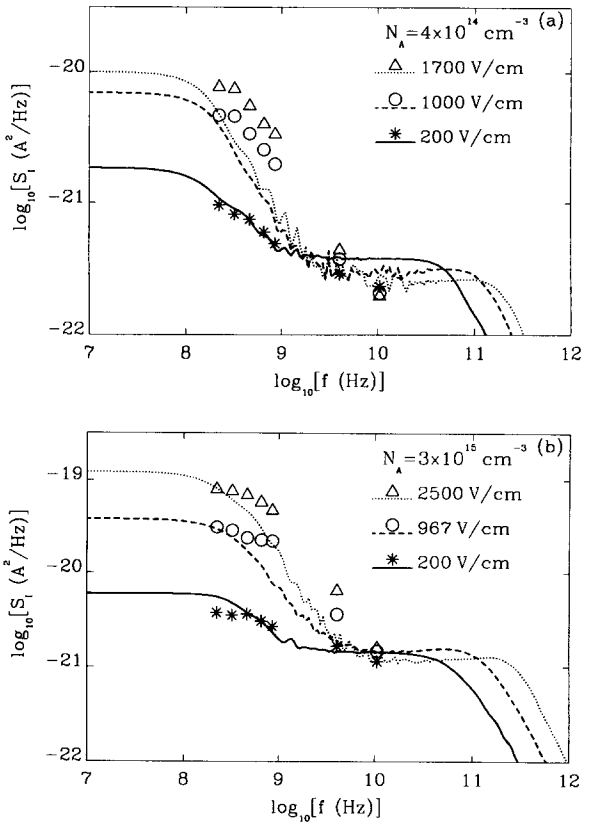

Fig. 1. Longitudinal component of the current spectral-density as a function of frequency at different electric field strengths in p-type Si at 77 K. Symbols refer to experiments, curves to MC calculation. (a) Refers to an acceptor concentrations $N_A = 4 \times 10^{14}\,\mathrm{cm}^{-3}$ with the fraction of ionized acceptors at thermodynamic equilibrium equal to 0·70. (b) Refers to $N_A = 3 \times 10^{15}\,\mathrm{cm}^{-3}$ with the fraction of ionized acceptors at thermodynamic equilibrium equal to 0·35.

the lowest frequencies. This excess noise vanishes for frequencies higher than the inverse of the carrier life-time, that is above about 2×10^8 Hz. Then the plateau associated with velocity fluctuations (in the presence of hot-carrier effects) is observed up to about 10^{11} Hz which represents the cut-off frequency of momentum relaxation rate. The increase of such cut-off frequency with increasing field reflects the decrease of the mobility which is associated with the onset of hot-carrier conditions.

4. Resistor

The system we consider is a submicron Si resistor of length $L = 0{\cdot}6\,\mu$m under extrinsic conditions with a donor concentration $N_D = 10^{17}\,cm^{-3}$ at 300 K. Figure 2 shows the voltage spectral density for the above resistor [42] calculated at several voltages. We remark that such a spectrum evidences the time scales associated with plasma and dielectric-relaxation effects, contrary to the case of current spectral density where the time scales associated with momentum and energy relaxation effects are detectable (see Fig. 1 at frequencies above the cut-off value for generation–recombination processes). Therefore, in the absence of the knowledge of the small-signal impedance spectrum, voltage and current spectral densities give complementary information. At low voltages plasma and differential dielectric-relaxation times are responsible for the peak at about $1{\cdot}2 \times 10^{12}$ Hz and the cut-off region, respectively. At increasing applied voltages, hot-carrier effects are present. Accordingly, the sublinear behavior of the current-voltage characteristics implies an increase of the differential resistance and, as a consequence, a significant increase of both: the low frequency value of $S_V(f)$ and of the dielectric relaxation time. This latter, by becoming longer than the plasma time, washes-out the plasma effects and, as seen in Fig. 2, the associated peak is found to disappear completely at the highest voltages.

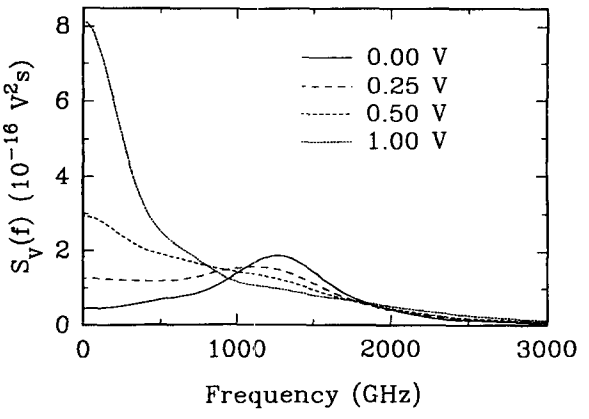

Fig. 2. Voltage spectral density in a homogeneous n-Si structure with $n = 10^{17}\,cm^{-3}$, $L = 0{\cdot}6\,\mu$m at $T_0 = 300$ K.

5. n^+nn^+ Structure

This is a very interesting structure, being the simplest non-homogeneous system and as such the prototype of most devices (two and three terminals). Therefore, in the following we will survey several situations which are considered to be of general interest: the long (over a few micron length) structure operating as a passive and active device, and the short (submicron length) structure. We consider first the case of a long n^+nn^+ structure made of GaAs at 300 K with the following parameters: length of the n-region $7{\cdot}5\,\mu$m, doping concentration in the n- and n^+-regions of $10^{15}\,cm^{-3}$ and $2 \times 10^{16}\,cm^{-3}$, respectively [52].

5.1 Passive device

The spectra of $S_I(f)$ and $\mathrm{Re}[Y(f)]$, calculated for several values of the applied voltages under the condition $\mathrm{Re}[Z(f)] > 0$ (passive device), are shown in Fig. 3a and b, respectively. At low voltages ($U < 1{\cdot}5$ V) both $S_I(f)$ and $\mathrm{Re}[Y(f)]$ remain nearly flat up to frequencies of about 100 GHz and then begin to decrease as $1/f^2$. The appearance of a resonant peak at $f = 1{\cdot}2$ THz reflects the existence of an additional noise-source related to the spontaneous fluctuations of single-carrier velocities at the nn^+ homojunctions with a frequency corresponding to the plasma frequency of an average electron concentration. A similar peak is also observed in the frequency dependence of $\mathrm{Re}Y[(f)]$. Since electron heating at the homojunctions is negligible, the frequency behavior of $S_I(f)$ and $\mathrm{Re}[Y(f)]$ at the resonant peak is practically independent from the applied voltage. When the potential approaches the threshold value, an additional resonant behavior of $S_I(f)$ and $\mathrm{Re}[Y(f)]$ appears in the intermediate frequency range $f = 20$–30 GHz. At $U = 2{\cdot}8$ V (i.e. slightly below the threshold value) negative

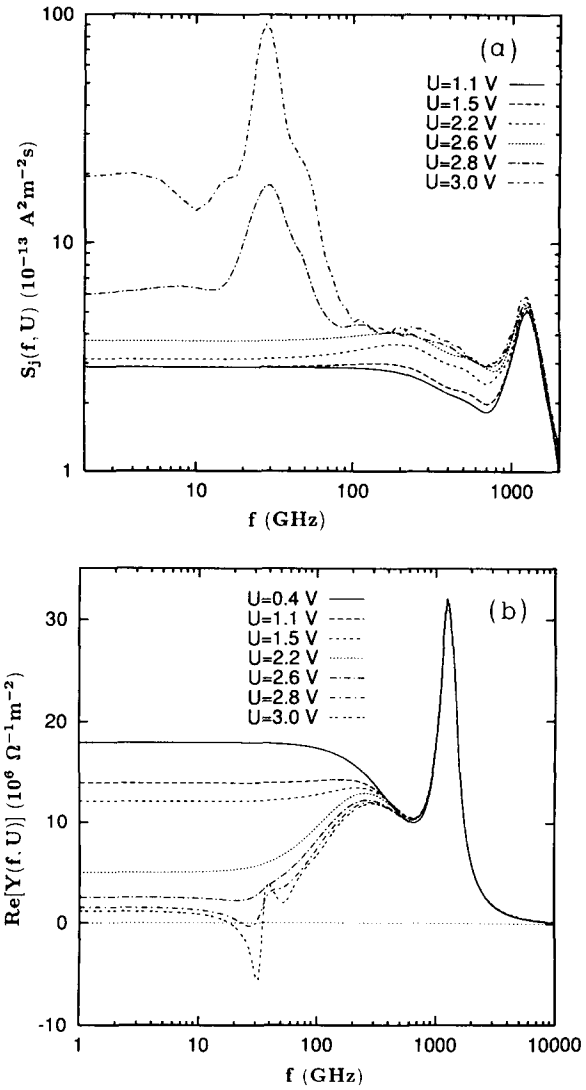

Fig. 3. Frequency dependence of: (a) the spectral density of current fluctuations; and (b) the real part of the small-signal admittance for an n^+nn^+ diode of GaAs with the length of the n-region of 7·5 μm, $n = 10^{15}$ cm^{-3}, $n^+ = 2 \times 10^{16}$ cm^{-3}, and $T_0 = 300$ K.

values of Re[$Y(f)$] appear in a narrow frequency range. The change in sign of Re[$Y(f)$] corresponds to the appearance of a second peak at lower frequency for $S_I(f)$ (see Fig. 3a, the curves for $U \geqslant 2{\cdot}8$ V). This second peak is associated with the spontaneous oscillations of the current at the transit-time frequency, where the oscillations are caused by the spontaneous formation of Gunn-domains and their subsequent drift through the n-region. The noise temperature corresponding to the results of Fig. 3a and b at 10 GHz is reported in Fig. 4 together with available experimental data [62]. The excellent agreement between theory and experiments proves the soundness of the theory and the reliability of the experiments.

5.2 Active device: amplifier

When Re[$Y(f)$] becomes negative inside a certain range of frequencies, which defines the amplification band, the two-terminal structure can be used for amplification or generation of electrical power within that band. In the case of an amplifier, the unloaded structure remains stable under current-mode operation [63, 64], hence, $Y(f)$ is a well-defined quantity. As a consequence, outside the amplification band, one can use eq. (7) for a theoretical calculation of $T_n(f)$. Analogously, an experimental investigation of $T_n(f)$ is also possible since, outside the amplification band, the impedance matching can be achieved with a proper choice of the output circuit parameters. However, inside the amplifi-

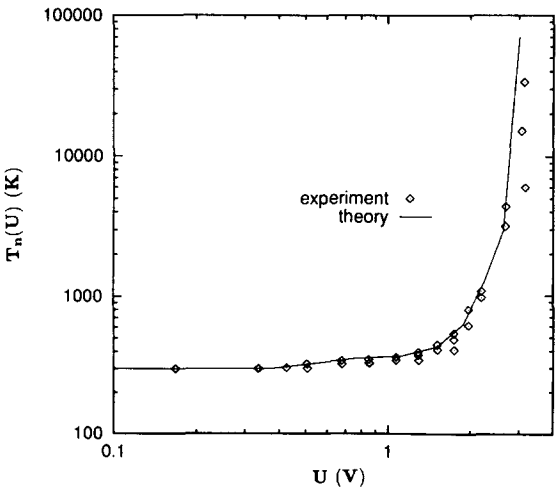

Fig. 4. Voltage dependence of the noise temperature at $f = 10$ GHz in the same diode of Fig. 3.

cation band the definition of the noise temperature given by eq. (7) has a drawback. Indeed, negative values of $\mathrm{Re}[Y(f)]$ would imply negative values of $T_n(f)$ which, in turn, can be interpreted as the possibility for the structure to become an active element (amplifier or generator) under suitable conditions [63, 64]. To describe the noise behavior of a stable active device inside the amplification band one can introduce the noise measure, $M(f)$, a dimensionless quantity defined as [65, 66]:

$$M(f) = \frac{S_I(f)}{4K_B T_0\{-\mathrm{Re}[Y(f)]\}} \tag{8}$$

where T_0 is the lattice temperature. The above quantity gives the intrinsic noise of an amplifier with shorted input. As a rule, under current-mode operation the above situation is realized when the value of the *nl* product (here *n* is the doping of the n-region and *l* its length) is sufficiently small for the self-generation to appear, and the electrical characteristics of the structure to remain stable in the whole region of applied voltage. Under voltage-mode operation, such a stable state of the active device can always be realized independently of the *nl* value, since any generation process is damped by the large external resistance of the supply circuit. Thus, for this operation mode the noise-temperature and noise-measure spectra defined, respectively, outside and inside the amplification band, can be numerically calculated or experimentally measured for any value of the voltage drop between the diode terminals, including the case when U is higher than the threshold value for Gunn-oscillations to appear under current-noise operation mode.

5.3 Active device: generator

In this case the structure goes into the self-oscillation regime for applied voltages above a threshold value (Gunn devices). This happens when the *nl* product is higher than some critical value which, for GaAs Gunn devices of several micrometer length, is of about $5 \times 10^{12}\,\mathrm{cm}^{-2}$. As a matter of fact, under current-noise operation mode the unloaded structure cannot achieve a stable state in the whole frequency range, as verified from both numerical simulations and experimental measurements. As a consequence, $Y(f)$ cannot be defined and eq. (7) fails. It should be mentioned that an intermediate situation between the amplifier and generator case can be realized for applied voltages slightly below the threshold for the Gunn-effect to occur. In this situation, the structure remains stable; however, being very near to becoming unstable, we can expect the appearance of some extra noise-source in its spectrum, as confirmed by calculations.

It should be noted that, in terms of the device small-signal impedance, $Z(f, U)$ (which remaining of finite magnitude is better suited than $Y(f, U)$ for the analysis of active devices), the amplifier and generator cases differ in the sign of $\mathrm{Im}[Z(f, U)]$ inside the amplification band. When $\mathrm{Im}[Z(f, U)]$ is negative, the structure remains stable under current-noise operation mode. When, at some frequency value inside the amplification band, $\mathrm{Im}[Z(f, U)] = 0$ and $(\mathrm{d}/\mathrm{d}f)\ \{\mathrm{Im}[Z(f, U)]\} > 0$, the resonant condition is fulfilled and the structure goes into self-oscillations without any external circuit [63, 64].

The noise-temperature spectrum, calculated in accordance with eq. (7), is shown in Fig. 5. At low voltages, below 0·4 V, $T_n(f)$ is practically independent from frequency and equals the lattice temperature, thus fulfilling the Nyquist theorem. Then, a systematic increase of $T_n(f)$ with U is observed. We remark that for frequencies near and above the plasma value (of about 1·3 THz) within the numerical uncertainty we have found $T_n \simeq T_0$ at all applied voltages. This means that this part of the $T_n(f)$ spectrum is caused mainly by electrons placed in n^+-regions. Thus, in the following we will focus our attention on frequencies below the plasma value. In the intermediate region $0{\cdot}4 < U < 1{\cdot}5$ V the increase of

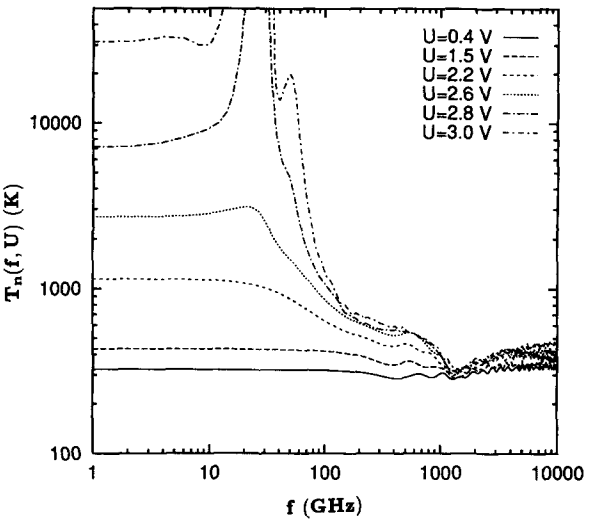

Fig. 5. Frequency dependence of the noise temperature for the same diode of Fig. 3 at several values of the applied voltage U.

$T_n(f)$ is smooth and mostly associated with the decrease of Re$[Y(f, U)]$. This behavior is due to carrier heating because of the high electric field inside the n-region (the average value ranges between 0·5 and 2 kV/cm). For voltages above about 1·5 V, heating is sufficient for carrier transfer to upper valleys. Accordingly, the increase of $T_n(f)$ with applied voltage becomes more pronounced and the spectrum exhibits a peculiar structure. The plateau at the lowest frequencies is followed by a bump evolving towards an asymptotic behavior in a small frequency region centered around the transit-time frequency $f = 25$ GHz. Then, in the high frequency range $(0{\cdot}2 < f < 1$ THz) $T_n(f)$ flattens taking values very similar to those of the electron temperature $T_e = 2 <\varepsilon>/(3K_B)$ in the n-region associated with the carrier average energy $<\varepsilon>$. For voltages up to 2·6 V, the increase of $S_I(U)$ plays a minor role when compared with the decrease of Re$[Y(U)]$, while above 2·6 V the increase of $S_I(U)$ also becomes quite significant. Then, due to the resonant behavior of both Re$[Y(f)]$ and $S_I(f)$ bump of $T_n(f)$ appears near the transit-time frequency. This bump quickly goes to infinity and the noise temperature becomes negative (thus it cannot be measured) inside the amplification band $f \equiv 15 \div 35$ GHz. At frequencies above the amplification band the noise temperature spectrum becomes positive again (and thus measurable). For example, one can detect the second peak of the noise temperature appearing near the frequency value of 50 GHz (see curve for $U = 3{\cdot}0$ V) that corresponds to the second harmonic of the transit-time frequency. Near the threshold value $U = 3{\cdot}1$ V (which corresponds to an average electric field of 4·2 kV/cm) the value of $T_n(f)$ at the lowest frequencies becomes practically infinity. This corresponds to the onset of electrical power self-generated at the frequency of about 25 GHz. Above this threshold voltage a noise temperature cannot be defined in the whole frequency range. It should be emphasized that below threshold voltage the above spectral behavior at the lowest frequencies is very similar to the usual noise temperature dependence on the electric field of the bulk material [67]. The noise-temperature spectrum for the amplifying device is rather complicated, especially at high voltages when several amplification bands appear. Inside the amplification bands the noise measure defined by eq. (8) can be used to characterize the noise properties of the amplifier. It should be stressed that eq. (8) is quite similar to eq. (7) when this latter is normalized to T_0. Therefore, both $T_n(f)/T_0$ and $M(f)$ are suitable quantities to characterize the noise of the same device. The advantage is that their spectra can be plotted on the same figure thus providing a noise figure of merit of the device operating in both the passive and active regions of the spectrum. The result of such a calculation for the amplifying structure at $U = 10$ V is reported in Fig. 6. Solid and dashed curves correspond to $T_n(f)/T_0$ and $M(f)$, respectively. For completeness, the dotted curve shows the frequency dependence of Re$[Y(f)]$ for the same device calculated with a hydrodynamic approach. We remark the minima of $M(f)$ at frequencies of about 18 and 36 GHz thus indicating the optimal frequencies of generation for the considered structure. By scaling the length of the

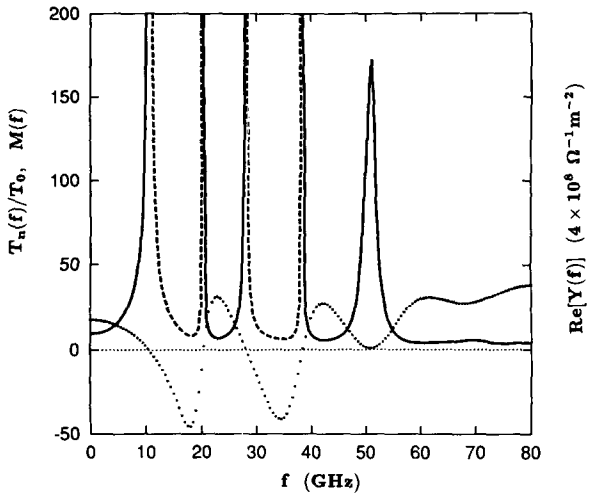

Fig. 6. Frequency dependence of the noise figure of merit for the same diode of Fig. 3 with $n = 2 \times 10^{14}\,cm^{-3}$ at $U = 10\,V$. Solid line refers to the relative noise temperature $T_n(f)/T_0$ and dashed line to the noise measure $M(f)$ defined for the amplifying device outside and inside the amplification band, respectively. Dotted line reports Re[$Y(f)$] calculated with a hydrodynamic approach.

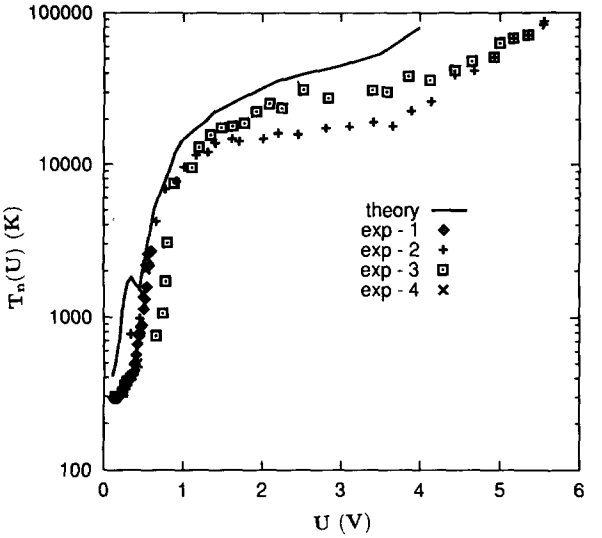

Fig. 7. Voltage dependence of the noise temperature at $f = 10\,GHz$ in a submicron diode of GaAs with the length of the n-region of $0{\cdot}2\,\mu m$, $n = 10^{17}\,cm^{-3}$ and $n^+ = 10^{18}\,cm^{-3}$, and $T_0 = 300\,K$.

structure down to the submicron region, the low-frequency plateau of both $S_I(f)$ and Re$Y[(f)]$ widens to higher frequencies [55]. This opens the possibility to investigate the noise temperature in submicron structures which remain stable up to sufficiently high values of the n-region doping even at applied voltages which correspond to average electric fields of several hundred kV/cm [60, 62, 68].

The results obtained for a length of the n-region of $0{\cdot}2\,\mu m$ and a doping $n = 10^{17}\,cm^{-3}$ are reported in Fig. 7 together with available experimental data [60, 62, 68]. The qualitative agreement between theory and experiments is considered to be satisfactory, having in mind that calculations are performed for a vertical rather than a planar structure as used in experiments. We remark that the absence of Gunn oscillations, typical of longer structures, makes possible the measurement of T_n up to voltages of 6 V under current operation-mode.

6. Schottky-barrier diode

The system we consider is a one-dimensional GaAs n^+–n–metal structure at 300 K [38]. The doping of the n^+-region is $10^{17}\,cm^{-3}$ and it is $0{\cdot}35\,\mu m$ long. At its left side, where the carriers are injected into the device, an ohmic contact is simulated, and the number of electrons considered is updated. The n-region is $0{\cdot}35\,\mu m$ long and its doping is $10^{16}\,cm^{-3}$. At its end it is the Schottky barrier with the metal contact acting as a perfect absorbing boundary. The height of the barrier considered in the simulation is 0·735 V, which leads to an effective built-in voltage between the n-region of the semiconductor and the metal of 0·640 V. The cross-sectional area adopted for the device is $2 \times 10^{-9}\,cm^2$, which means an average number of simulated carriers around 7600 depending on the bias. Figure 8 shows $S_I(f)$ at increasing applied voltages. Two peaks are observed, one in the region below 10^3 GHz and another at about $2{\cdot}2 \times 10^3$ GHz. The first is attributed to carriers that have insufficient kinetic energy to surpass the barrier and

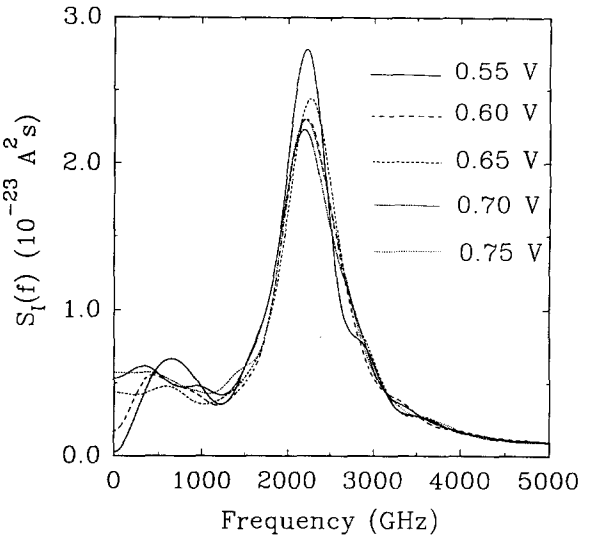

Fig. 8. Current spectral-density for a GaAs Schottky barrier diode at $T_0 = 300$ K with $n = 10^{16}$ cm^{-3}, $n^+ = 10^{17}$ cm^{-3} and length of each region of 0·35 μm.

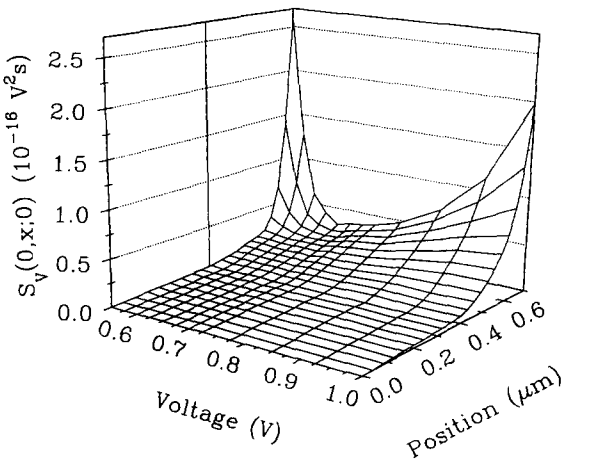

Fig. 9. Low-frequency value of the spectral density of voltage fluctuations as a function of position and mean voltage in the same structure as Fig. 8. The semiconductor-metal contact is at $x = 0{\cdot}7$ μm.

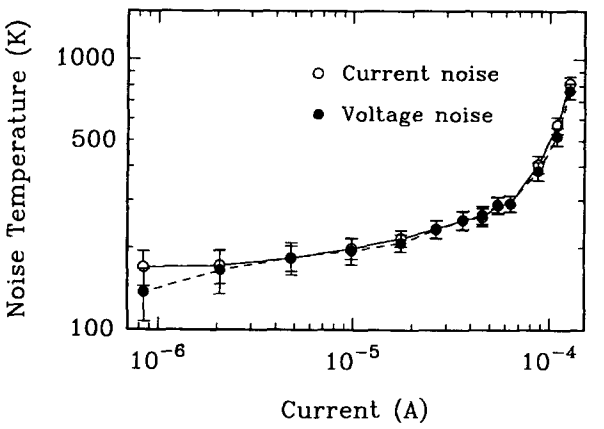

Fig. 10. Noise temperature at low frequency as a function of current for the Schottky-barrier diode of Fig. 8. Full and open circles refer to voltage–noise and current–noise operations, respectively.

return to the neutral semiconductor region. The second originates from the coupling between fluctuations in carrier velocity and in self-consistent field due to the n^+n homojunction as discussed for the n^+nn^+ structure. Figure 9 shows a spatial analysis of the low-frequency value of the voltage spectral density. For voltages lower than 0·640 V shot-noise is dominant, and most of the noise arises in the depletion region close to the barrier. At increasing voltages, thermal noise associated with the series resistance prevails, and the noise becomes spatially more distributed, mainly originating from the n-region of the device. At the highest voltages, the presence of hot-carriers and intervalley mechanisms in the n-region leads to the appearance of an excess noise. Figure 10 reports the equivalent noise temperature at low frequency calculated for both current and voltage operation modes. (We remark the interesting property of the noise temperature whose value is independent from the operation mode.) For low currents, corresponding to the exponential region of the current-voltage characteristic, the noise temperature is close to half the value of the lattice temperature. This reveals a full shot-noise behavior $S_I(0) = 2eI$. As the current increases, the effect of the thermal noise in the series resistance becomes important and the noise temperature increases towards the lattice temperature, which is clearly crossed over for the highest currents because of the onset of the hot-carrier effects described before. This behavior of

$T_n(0)$ agrees well with that found by different experimental results [69–72]. We remark on the great influence of the coupling between fluctuations in carrier velocity and self-consistent electric field in determining the noise properties of these devices.

7. MESFET

The noise analysis has been carried out for a GaAs MESFET consisting of an n^+nn^+ structure with a 1 μm channel modulated by a gate contact of 0·5 μm. A two-dimensional vertical structure is considered, the source and drain contacts being 0·2 μm long and placed at the end of the n^+-regions. The doping of the n-region is of $4 \times 10^{16}\,cm^{-3}$ and that of the source and drain regions of $10^{17}\,cm^{-3}$ (about a factor 10 lower than in the practical case to keep acceptable computational times). In order to compute fluctuations in a two-dimensional geometry, we have used an appropriate generalization of the Ramo-Shockley theorem given in [73]. By adopting voltage-noise operation, we can take advantage of analyzing the drain-voltage fluctuations and their spatial origin [37]. Figure 11 shows the low-frequency value of the spectral density of voltage fluctuations (as measured from the source contact), $S_V(x, y; f)$, as a function of the position inside the MESFET for fixed values of V_{GS} and I_D corresponding to the conditions of equilibrium ($V_{GS} = -0{\cdot}5\,V$, $I_D = 0$) and saturation ($V_{GS} = -0{\cdot}5\,V$, $I_D = 91{\cdot}1\,A/m$). Here the spatial distribution of the voltage noise can be clearly observed. We notice that in the drain contact the value of the spectral density must be the same for all the y positions, and in the gate contact must be null since its voltage is kept constant in time. Figure 12 shows the spectral density of voltage fluctuations along the channel in the y position corresponding to 0·096 μm as a function of frequency and x position for the MESFET at the operating point corresponding to saturation. Here it can be clearly observed that the increase in the drain voltage noise takes place mainly at the lowest frequencies (between 0 and 30 GHz) and is localized between the gate and the drain; the penetration in the drain n^+-region being less pronounced as the frequency increases. The most important figure of merit for a MESFET is the minimum noise-figure, which characterizes the degradation of the signal-to-noise ratio within the input and output of the transistor at a given frequency. Figure 13 reports the intrinsic minimum noise-figure of the MESFET here analyzed under the conditions $V_{GS} = -0{\cdot}25\,V$, $V_{DS} = 1{\cdot}5\,V$ and $V_{GS} = -1{\cdot}0\,V$, $V_{DS} = 1{\cdot}5\,V$, respectively. The calculated noise-figure exhibits the well-known behavior found from experiments. It starts from zero and systematically increases with frequency for both the considered operation points, higher values being associated with higher drain currents. For comparison, results using the algorithm of [22] have been reported in the same figure. The lowest values obtained by [22] are attributed to the approximation there introduced of neglecting the frequency dispersion of the spectral density of the gate-current fluctuations.

8. Conclusions

We have surveyed some interesting results concerning the Monte Carlo analysis of electronic noise in semiconductor materials and devices performed in recent years. The main advantage of such an approach is in avoiding unjustified or phenomenological approximations in modeling carrier transport in devices, thus providing an exact solution of the appropriate master equation self-consistently coupled with a Poisson solver. In this way, fluctuations are treated on the same microscopic level as for the case of kinetic coefficients (e.g. mobility, diffusivity, etc.) without invoking phenomenological noise-sources. Current-noise operation mode, by allowing a decomposition in terms of different noise contributions, is found to provide useful information on the nature of different noise sources. Accordingly, fluctuations related to generation-recombination, velocity, energy, long-range Coulomb interactions (plasma effects), etc.

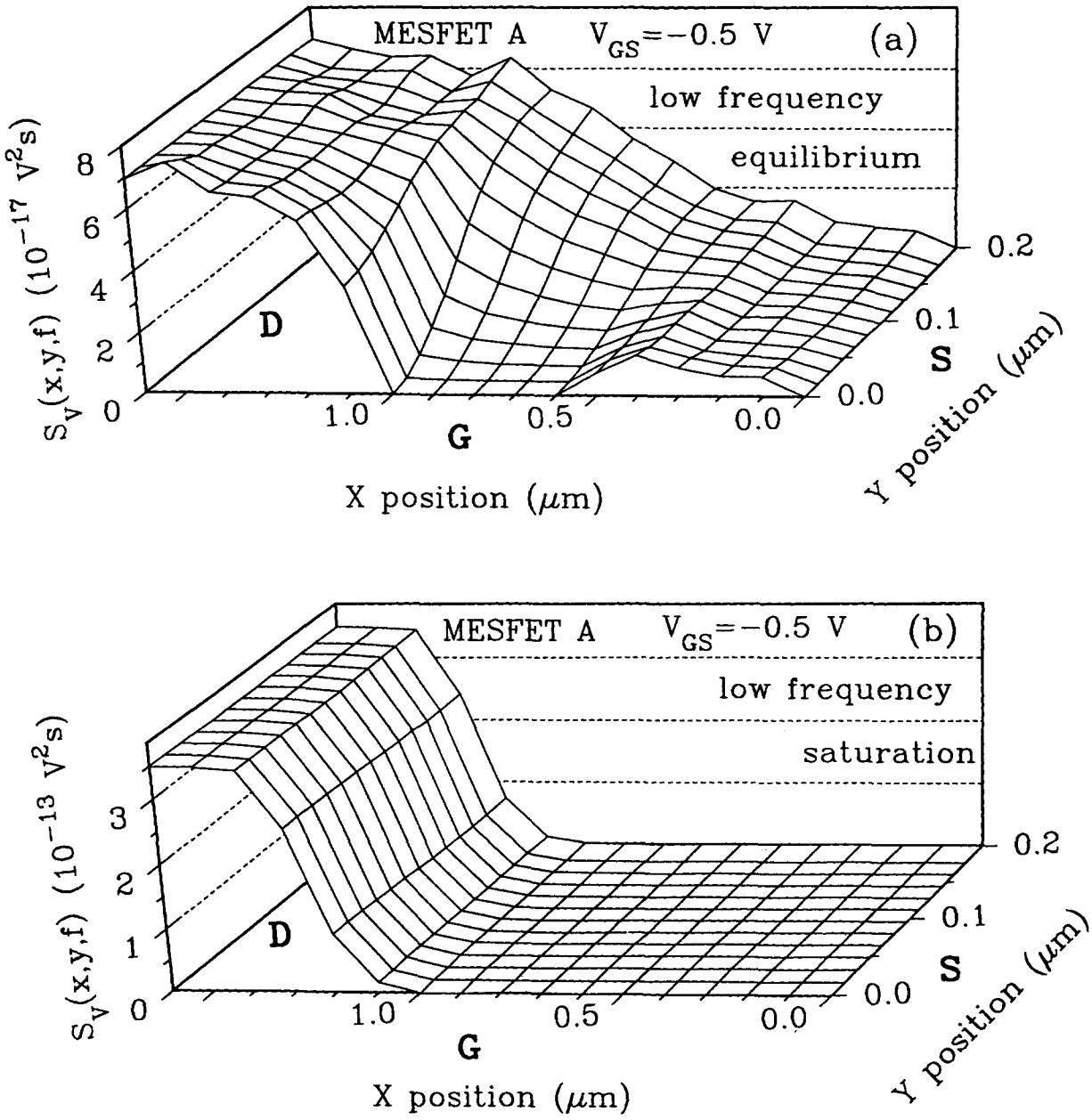

Fig. 11. Spatial map inside the MESFET of the low-frequency value of the spectral density of voltage fluctuations (with respect to the source) for two bias point: (a) equilibrium, $V_{GS} = -0{\cdot}5$ V, $I_D = 0$ (average drain voltage of 0 V); (b) saturation $V_{GS} = -0{\cdot}5$ V, $I_D = 91{\cdot}1$ A/m (average drain voltage of 1·3 V). The positions of the source (S), gate (G) and drain (D) are indicated in the figure.

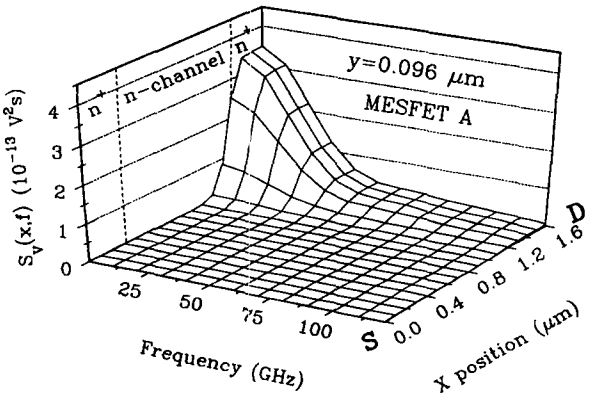

Fig. 12. Spectral density of voltage fluctuations (with respect to the source) as a function of frequency and x position for a fixed y position corresponding to 0·096 μm in MESFET at the operating point $V_{GS} = -0{\cdot}5$ V, $I_D = 91{\cdot}1$ A/m (average drain voltage of 1·3 V). The positions of the source (S), gate (G) and drain (D) are indicated in the figure.

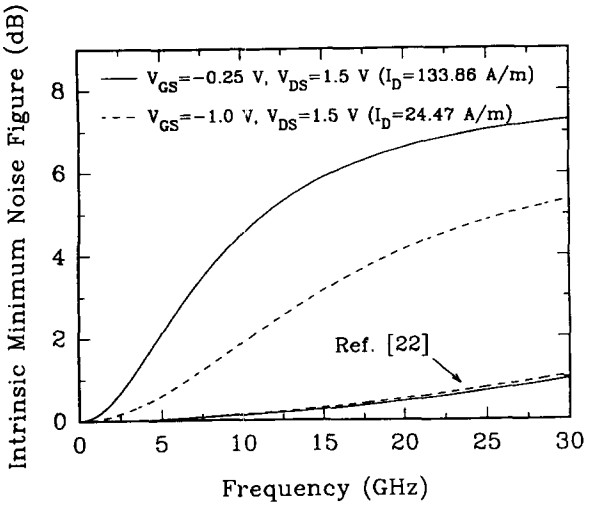

Fig. 13. Intrinsic minimum noise-figure of the MESFET of Fig. 11 for the reported operation points. Results obtained using the algorithm of [22] are also reported for comparison.

together with the respective cross-correlations can be identified. Voltage–noise operation mode, by allowing a spatial analysis to be carried out, is found to provide local information on the strength of the noise sources. The systems investigated, by including high electric fields, spatial non-homogeneities, three terminal devices, provide the reader with a sufficiently wide scenario of noise in semiconductor materials and devices. Quality and reliability factors have been quantitatively evaluated with the help of the noise-temperature and noise-measure concepts as well as of the minimum noise-figure for the cases of two and three terminal devices, respectively. The major drawback of the Monte Carlo approach rests on the need for long computational times and an accurate knowledge of the microscopic parameters entering the modeling. Nevertheless, we believe that the generality of such an approach opens wide possibilities for further developments towards an implementation of the numerical codes which makes possible the analysis of more complicated systems.

Acknowledgements

This work has been performed within the European Laboratory for Electronic Noise (ELEN) supported by the Commission of European Community through the contract EKBXCT920047 and the PECO Project EAST ELEN ERBCIPDCT940020. Partial support from the Comisión Interministerial de Ciencia y Tecnología (CICYT) through the project TIC95-0652 and from a NATO Networking Infrastructure Grant 951009 is acknowledged.

References

[1] *Proceedings of the 6th Int. Conf. on Noise in Physical Systems and 1/f Noise*, P.H.E. Meijer, R.D. Mountain and R.J. Soulen (eds), National Bureau of Standards, Washington, 1981.

[2] *Proceedings of the 7th Int. Conf. on Noise in Physical Systems and 1/f Noise*, M. Savelli, G. Lecoy and J.P. Nougier (eds), North-Holland, Amsterdam, 1983.

[3] *Proceedings of the 8th Int. Conf. on Noise in Physical Systems and 1/f Noise*, A. Amico and P. Mazzetti (eds), North-Holland, Amsterdam, 1985.

[4] *Proceedings of the 9th Int. Conf. on Noise in Physical Systems and 1/f Noise*, C.M. Van Vliet (ed.), World Scientific, New York, 1987.

[5] *Proceedings of the 10th Int. Conf. on Noise in Physical Systems and 1/f Noise*, A. Ambrozy (ed.), Akademiai Kiado, Budapest, 1989.
[6] *Proceedings of the 11th Int. Conf. on Noise in Physical Systems and 1/f Noise*, T. Musha, S. Sato and M. Yamamoto (eds), Ohmsha Ltd, Kyoto, 1991.
[7] *Proceedings of the 12th Int. Conf. on Noise in Physical Systems and 1/f Noise*, P.H. Handel and A.L. Chung (eds), AIP Press, New York, 1993.
[8] *Proceedings of the 13th Int. Conf. on Noise in Physical Systems and 1/f Noise*, V. Bareikis and R. Katilius (eds), World Scientific, Palanga, 1995.
[9] L.K.J. Vandamme, Noise as a diagnostic for quality and reliability of electronic devices, *IEEE Trans. Electron Devices*, ED-41 (1994) 2176.
[10] K.M. Van Vliet, Markov approach to density fluctuations due to transport and scattering. I. Mathematical formalism, *J. Math. Phys.*, 12 (1971) 1981; II. applications, *Ibid.*, 12 (1971) 1998.
[11] Van Kampen, *Stochastic Processes in Physics and Chemistry*, North Holland, Amsterdam, 1981.
[12] L. Reggiani, P. Lugli and V. Mitin, Generalization of Nyquist–Einstein relationship to conditions far from equilibrium in non-degenerate semiconductors, *Phys. Rev. Lett.*, 8 (1988) 736.
[13] W. Fawcett, A.D. Boardman and S. Swain, Monte Carlo determination of electron transport properties in gallium arsenide, *J. Phys. Chem. Solids*, 31 (1970) 1963.
[14] P.J. Price, Monte Carlo calculation of electron transport in solids, in *Semiconductor and Semimetals*, Vol. 14, R.K. Willardson and A.C. Beer (eds), Academic Press, New York, 1979, p. 249.
[15] C. Jacoboni and L. Reggiani, The Monte Carlo method for the solution of charge transport in semiconductors with application to covalent materials, *Rev. Mod. Phys.*, 55 (1983) 645.
[16] R.W. Hockney and J.W. Eastwood, *Computer Simulation using Particles*, Adam Hilger, Bristol, 1988.
[17] C. Jacoboni and P. Lugli, The Monte Carlo method for semiconductor simulation, *Springer Series on Computational Microelectronics*, S. Selberherr (ed.), Springer, New York, 1989.
[18] J. Zimmerman and E. Constant, Application of Monte Carlo techniques to hot carrier diffusion noise calculation in unipolar semiconducting components, *Solid State Electron.*, 23 (1980) 914.
[19] R. Grondin, P.A. Blakey, J.R. East and E.D. Rothman, Monte Carlo estimation of hot carrier noise at millimeter- and submillimeter wave frequencies, *IEEE Trans. Electron Devices*, ED-28 (1981) 914.
[20] B. Boittiaux, E. Constant and A. Ghis, Simulation of diffusion noise in a device, *Proceedings of the 7th Int. Conf. on Noise in Physical Systems and 1/f Noise*, M. Savelli, G. Lecoy and J.P. Nougier (eds), Amsterdam, 1983, p. 19.
[21] C. Moglestue, Monte Carlo modelling of noise in semiconductors, *Proceedings of the 7th Int. Conf. on Noise in Physical Systems and 1/f Noise*, M. Savelli, G. Lecoy and J.P. Nougier (eds), Elsevier, Amsterdam, 1983, p. 23.
[22] C. Moglestue, A Monte Carlo particle study of the intrinsic noise figure in GaAs MESFETs, *IEEE Trans. Electron. Devices*, ED-32 (1985) 2092.
[23] P. Lugli and L. Reggiani, Electron–electron interaction effect on the spectral density of current fluctuations of hot electrons in Si, *Proceedings of the 8th Int. Conf. on Noise in Physical Systems and 1/f Noise*, A. D'Amico and P. Mazzetti (eds), North-Holland, Amsterdam, 1985, p. 235.
[24] B.R. Nag, S.R. Ahmed and M. Deb Roy, Noise current spectrum in submicrometer samples, *Appl. Phys.*, A 41 (1986) 197.
[25] L. Reggiani, P. Lugli and V. Mitin, Monte Carlo algorithm for generation recombination in semiconductors, *Appl. Phys. Lett.*, 51 (1987) 925.
[26] D. Junevicius and A. Retlaitis, Monte Carlo particle investigation of noise in short n^+nn^+ GaAs diodes, *Electronic Lett.*, 24 (1988) 1307.
[27] T. Kuhn, L. Reggiani, L. Varani and V. Mitin, Monte Carlo method for the simulation of electronic noise in semiconductors, *Phys. Rev.*, B42 (1990) 5702.
[28] T. Kuhn, L. Reggiani and L. Varani, Correlation functions and electronic noise in doped semiconductors, *Phys. Rev.*, B42 (1990) 11133.
[29] J. Gest, H. Fawaz, H. Kabbaj and J. Zimmermann, Microwave hot electron noise power and two-dimensional electron diffusion coefficient in AlGaAs-GaAs MODFETs, in *Noise in Physical systems and 1/f Fluctuations*, T. Musha, S. Sato and M. Yamamoto (eds), Ohmsha Ltd, 1991, pp. 291–295.
[30] T. Kuhn, L. Reggiani, L. Varani, D. Gasquet, J.C. Vaissiere and J.P. Nougier, Field dependent electronic noise of lightly doped p-type Si at 77 K, *Phys. Rev.*, B44 (1991) 1074.
[31] L. Varani, L. Reggiani, P. Houlet and T. Kuhn, Shot noise in hot carrier transport, *Proc. 21st I.C.P.S.*, P. Jiang and H.Z. Zheng (eds), World Scientific, Singapore, 1992, p. 333.
[32] J.G. Adams and T. Tang, Monte Carlo simulation of noise in GaAs at electric fields up to the critical field, *IEEE Electron Device Lett.*, EDL-13 (1992) 378.
[33] L. Reggiani, T. Kuhn and L. Varani, Noise and correlation functions of hot carriers in semiconductors, *Appl. Phys. A*, 54 (1992) 411.
[34] V. Gružinskis, E. Starikov, P. Shiktorov, L. Reggiani, M. Saraniti and L. Varani, Response functions for submillimeter n^+nn^{++} diode generators, *Lith. J. Phys.*, 32 (5) (1992) 169.
[35] L. Varani, T. Kuhn, L. Reggiani and Y. Perles, Current and number fluctuations in submicron

n^+nn^{++} structures, *Solid State Electron.*, 36 (1993) 251.

[36] T. Gonzalez and D. Pardo, Ensemble Monte Carlo with Poisson solver for the study of current fluctuations in homogeneous GaAs structures, *J. Appl. Phys.*, 73 (1993) 7453.

[37] T. Gonzalez, D. Pardo, L. Varani and L. Reggiani, Spatial analysis of electronic noise in submicron semiconductor structures, *Appl. Phys. Lett.*, 63 (1993) 84.

[38] T. Gonzalez, D. Pardo, L. Varani and L. Reggiani, Monte Carlo analysis of noise spectra in Schottky-barrier diodes, *Appl. Phys. Lett.*, 63 (1993) 3040.

[39] T. Gonzalez, D. Pardo, L. Varani and L. Reggiani, The microscopic interpretation of electronic noise in Schottky-barrier diodes, *ESSDERC'93*, 1993, p. 3040.

[40] K.Y. Lee, H.S. Min and Y.J. Park, Estimation of noise power spectral densities from the Monte Carlo simulated terminal currents in semiconductor devices, *Solid State Electron.*, 36 (1993) 1563.

[41] L. Varani and L. Reggiani, Microscopic theory of electronic noise in semiconductor unipolar structures, *Rivista Nuovo Cimento*, 17 (7) (1994).

[42] L. Varani, L. Reggiani, T. Kuhn, T. Gonzalez and D. Pardo, Microscopic simulation of electronic noise in semiconductor materials and devices, *IEEE Trans. Electron. Devices*, 41 (1994) 1916.

[43] V. Gruzhinskis, E. Starikov, P. Shiktorov, R. Gricius, V. Mitin, L. Reggiani and L. Varani, Noise and impedance of submicron InP diodes, *Proc. European Gallium Arsenide and Related III–V Compounds Applications Symposium*, 28–30 April 1994, Politecnico di Torino, Italy, p. 365.

[44] V. Gruzhinskis, V. Mitin, E. Starikov and P. Shiktorov, Noise and impedance of n^+nn^{++} InP microwave generators, *J. Appl. Phys.*, 75 (1994) 8210.

[45] J.G. Adams, T.W. Tang and L.E. Kay, Monte Carlo simulation of noise in GaAs semiconductor devices, *IEEE Trans. Electron Devices*, 41 (1994) 575.

[46] V. Gruzhinskis, E. Starikov and P. Shiktorov, Monte Carlo simulation of hot carrier noise in short n^+nn^{++} diodes, *Physica Scripta*, T54 (1994) 146.

[47] V. Gruzhinskis, E. Starikov, P. Shiktorov, R. Gricius, V. Mitin, L. Reggiani and L. Varani, Electronic noise and impedance field of submicron n^+nn^{++} InP diode generators, *Semicond. Sci. Technol.*, 9 (1994) 1843.

[48] V. Gružinskis, E. Starikov, P. Shiktorov, L. Reggiani, L. Varani, J.C. Vaissiere, J.P. Nougier, P. Houlet and L. Hlou, Monte Carlo simulation of hot carrier noise in short n^+nn^{++} diodes, *Proc. 7th Vilnius Conf. on Fluctuation Phenomena in Physical Systems*, V. Palenskis (ed.), Vilnius Univ. Press, 1994, p. 205.

[49] V. Gružinskis, E. Starikov, P. Shiktorov, V. Mitin, L. Reggiani, L. Varani, J.C. Vaissiere, J.P. Nougier, P. Houlet, L. Hlou and D. Gasquet, A novel procedure to obtain the small-signal characteristics of a given device from noise spectra, *Proc. 7th Vilnius Conf. on Fluctuation Phenomena in Physical Systems*, V. Palenskis (ed.), Vilnius Univ. Press, 1994, p. 211.

[50] T. Gonzalez, D. Pardo, L. Varani and L. Reggiani, Monte Carlo analysis of the behavior and spatial origin of electronic noise in GaAs MESFETs, *IEEE Trans. Electron Devices*, 42 (1995) 991.

[51] E. Starikov, P. Shiktorov, V. Gružinskis, J.P. Nougier, J.C. Vaissiere, L. Varani and L. Reggiani, Electronic noise of submicron n^+nn^{++} diodes under near-oscillatory macroscopic behaviors, *Appl. Phys. Lett.*, 66 (1995) 2361.

[52] V. Gružinskis, E. Starikov, P. Shiktorov, L. Reggiani and L. Varani, Modelling of noise–temperature measurements in submicrometer semiconductor structures, *Proc. of the 13th Int. Conf. on Noise in Physical Systems and 1/f fluctuations*, V. Bareikis and R. Katilius (eds), World Scientific, 1995, p. 177.

[53] V. Gružinskis, E. Starikov, P. Shiktorov, L. Reggiani, J.C. Vaissiere, J.P. Nougier, L. Varani, P. Houlet and D. Gasquet, Monte Carlo simulation of hot carrier noise in submicron n^+nn^{++} diodes, *Proc. of 13th International Conference on Noise in Physical Systems and 1/f Fluctuations*, V. Bareikis and R. Katilius (eds), World Scientific, Singapore, 1995, p. 189.

[54] V. Gružinskis, E. Starikov and P. Shiktorov, Hydrodynamic and kinetic modelling of hot carrier noise in n^+nn^{++} GaAs diodes, *Lith. J. Phys.*, 35 (1995) 445.

[55] E. Starikov, P. Shiktorov, V. Gružinskis, J.P. Nougier, J.C. Vaissiere, L. Varani and L. Reggiani, Monte Carlo calculation of noise and small-signal impedance spectra in submicrometer GaAs n^+nn^{++} diodes, *J. Appl. Phys.*, 79 (1996) 242.

[56] A. Van der Ziel, *Noise in Solid State Devices and Circuits*, Wiley, New York, 1986.

[57] W. Shockley, Current to conductors induced by a moving point charge, *J. Appl. Phys.*, 9 (1938) 635.

[58] S. Ramo, Currents induced by electron motion, *Proc. I.R.E.*, 27 (1939) 584.

[59] B. Pellegrini, Electrical charge motion, induced current, energy balance, and noise, *Phys. Rev.*, B34 (1986) 5921.

[60] V. Bareikis, J. Liberis, I. Matulieniene, A. Matulionis and P. Sakalas, Experiments on hot electron noise in semiconductor materials for high-speed devices, *IEEE Trans. Electron. Devices*, ED-41 (1994) 2050.

[61] P.J. Price, Fluctuations of hot electrons, in *Fluctuation Phenomena in Solids*, R.E. Burgess (ed.), Academic Press, New York, 1965, p. 355.

[62] V. Bareikis, J. Liberis, I. Matulieniene, A. Matulionis, A. Oginskis, P. Sakalas and R. Šaltis, Hot electron noise temperature in n-type GaAs channel at fields

over 100 kV/cm, *Proc. 7th Vilnius Conf. Fluct. Phenom. Phys. Syst.*, V. Palenskis (ed.), Vilnius Univ. Press, 1994, p. 217.

[63] V. Gružinskis, E. Starikov and P. Shiktorov, Impedance and microwave power generation in short n^+nn^{++} InP diodes, *Liet. Fiz. Žurn.*, 34 (1994) 254.

[64] V. Gružinskis, E. Starikov, P. Shiktorov, L. Reggiani, M. Saraniti and L. Varani, Generation and amplification of microwave power in submicron n^+nn^{++} diodes, *Simulation of Semiconductor Devices and Processes*, Vol. 5, S. Selberherr, H. Stippel and E. Strasser (eds), 1993, p. 333.

[65] B.C. DeLoach, The noise performance of negative conductance amplifier, *IRE Trans. Electron. Devices, ED-9 (1962) 366.*

[66] H.K. Gummel and J.L. Blue, A small-signal theory of avalanche noise in IMPATT diodes, *IEEE Trans. Electron. Devices*, ED-14 (1967) 569.

[67] E. Starikov, P. Shiktorov, V. Gružinskis, L. Reggiani, L. Varani, J.C. Vaissiere and J.P. Nougier, Hydrodynamic and kinetic modelling of hot-carrier noise temperature in bulk semiconductors, *Lith. J. Phys.*, 35 (1995) 408.

[68] V. Aninkevičisu, V. Bareikis, R. Katilius, J. Liberis, I. Matulionine, A. Matulionis, P. Sakalas and R. Šaltis, Hot electron noise in GaAs at extremely high electric fields, in *Noise in Physical Systems and 1/f Fluctuations*, V. Bareikis and R. Katilius (eds), World Scientific, Singapore, 1995, p. 173.

[69] M. Trippe, G. Bosman and A. van der Ziel, Transit-time effects in the noise of Schottky-barrier diodes, *IEEE Trans. Microw. Theory Tech.*, 34 (1986) 1183.

[70] E. Kollberg, H. Zirath and A. Jelenski, Temperature-variable characteristics and noise in metal-semiconductor junctions, *IEEE Trans. Microw. Theory Tech.*, 34 (1986) 913.

[71] A. Jelenski, E. Kollberg and H. Zirath, Broad-band noise mechanisms and noise measurements of metal–semiconductor junctions, *IEEE Trans. Microw. Theory Tech.*, 34 (1986) 1193.

[72] S. Palczewski, A. Jelenski, A. Grüb and H. Hartnagel, Noise characterization of Schottky barrier diodes for high-frequency mixing applications, *IEEE Microw. Guid. Wave Lett.*, 2 (1992) 442.

[73] V. Gružinskis, S. Kersulis and A. Reklaitis, An efficient Monte Carlo particle technique for two-dimensional transistor modeling, *Semicond. Sci. Technol.*, 6 (1991) 602.